

Fig. 3 Optical spectrum of compressed pulse which has been broadened from 1.3nm to greater than 6nm due to SPM

axes) of the fibre are also very crucial. Therefore, a polarisation controller is used at the fibre input to control the input polarisation state of the light into the fibre.

The intensity discrimination relies on the intensity dependent polarisation state of light in fibre. As the optical pulse propagates in the fibre, the narrowing process caused by the soliton effect starts which increases the pulse peak power. The compressed pulse consists of a high intensity peak and a low intensity pedestal. Owing to the intensity-dependent nonlinear birefringence, the intense central peak and the weak pedestal experience different phase shifts, depending on their power levels. Consequently the high intensity peak and low intensity pedestal will have different polarisation states at the fibre output. At appropriate power levels, the phase shift of the intense central peak can be fully compensated for and changed to the linear polarisation state with the quarter wave plate while leaving the pedestal components in a different polarisation state. Subsequently, with the help of a polariser, intensity discrimination against the pedestal can be realised.

In this experiment, for eighth order solitons, we successfully suppressed the pedestal and achieved clean high quality 185fs pulses. Fig. 4 shows the autocorrelation trace of the pulses after passing through the polariser, which clearly shows that the inherently associated pedestal component has been removed. This was also confirmed by autocorrelation measurements at a much larger time scale (total time delay of >30ps). These represent the shortest pedestal-free pulses ever generated from semiconductor lasers. This technique of wing suppression was applied at different soliton orders. It was found that at higher soliton orders, although the pulse width could be even shorter, pedestal suppression was not as effective as that for eighth order solitons. This can be attributed to the fact that the optimum fibre length for higher order solitons was too short to cause appropriate phase shifts between the peak and the pedestal components. However, with further optimisation of fibres, we believe pedestal-free pulses with even shorter widths can be generated.

Conclusions: We have demonstrated a novel technique for simultaneous optical pulse compression and pulse reshaping, which can significantly improve the pulse quality achieved by the soliton-effect pulse compression. A very simple and practically viable experimental setup has been used to generate 185fs high-quality pedestal free pulses from a semiconductor laser.

Acknowledgments: Photonics Research Laboratory is a member of the Australian Photonics Cooperative Research Centre. This work is partly supported by the Australian Research Council.

© IEE 1995

18 November 1994

Electronics Letters Online No: 19950123

K.A. Ahmed, H.H.Y. Cheng and H.F. Liu (Photonics Research Laboratory, Department of Electrical & Electronic Engineering, The University of Melbourne, Parkville, Victoria 3052, Australia)

References

- POTASEK, M.J.: 'Novel femtosecond solitons in optical fibers, photonics switching, and computing', *J. Appl. Phys.*, 1989, **65**, pp. 941-953
- LIU, H.F., OGAWA, Y., OSHIBA, S., and NONAKA, T.: 'Picosecond pulse generation from a 1.3mm distributed feedback laser diode using soliton-effect compression', *IEEE J. Quantum Electron.*, 1991, **QE-27**, pp. 1655-1660
- ONG, J.T., TAKAHASHI, R., TSUCHIYA, M., WONG, S.H., SAHARA, R.T., OGAWA, Y., and KAMIYA, T.: 'Subpicosecond soliton compression of gain-switched diode laser pulses using an erbium-doped fibre amplifier', *IEEE J. Quantum Electron.*, 1993, **QE-29**, pp. 1701-1707
- NAKAZAWA, M., SUZUKI, K., and YAMADA, E.: 'Femtosecond pulse generation using a distributed feedback laser diode', *Electron. Lett.*, 1990, **26**, pp. 2038-2041
- CHUSSEAU, L., and DELEVAQUE, E.: '250-fs optical pulse generation by simultaneous soliton compression and shaping in a nonlinear optical loop mirror including a weak attenuation', *Opt. Lett.*, 1994, **19**, pp. 734-736
- STOLEN, R.H., BOTINEAU, J., and ASHKIN, A.: 'Intensity discrimination of optical pulses with birefringent fibers', *Opt. Lett.*, 1982, **7**, pp. 512-514
- AHMED, K.A., LIU, H.F., ONODERA, N., LEE, P., TUCKER, R.S., and OGAWA, Y.: 'Nearly transform-limited pulse (3.6) generation from gain-switched 1.55µm distributed feedback laser by using fibre compression technique', *Electron. Lett.*, 1993, **29**, pp. 54-55

High efficiency AlGaInP-based 660-680nm vertical-cavity surface emitting lasers

M. Hagerott Crawford, R.P. Schneider, Jr.,
K.D. Choquette, K.L. Lear, S.P. Kilcoyne and
J.J. Figiel

Indexing terms: Vertical cavity surface emitting lasers, Visible semiconductor lasers

Record continuous-wave output power of 2.9mW and 10% peak wallplug efficiency have been achieved from planar gain guided AlGaInP-based vertical-cavity surface emitting lasers. These results represent nearly an order of magnitude improvement in performance over previous AlGaInP-based vertical-cavity lasers.

Vertical cavity surface emitting lasers (VCSELs) are well suited to many optoelectronic applications due to the low divergence output beams and amenability to two dimensional arrays. VCSELs that emit in the visible region of the spectrum in particular are of interest for applications such as plastic fibre based optical communications, laser printing and optical data storage. Recent progress in the development of visible VCSELs includes the demonstration of continuous wave (CW) room temperature lasing in the 650-680 nm range from VCSELs with AlGaInP quantum well active regions and AlGaAs distributed Bragg reflectors (DBRs) [1]. The best performance for these structures was achieved from planar gain guided devices with an 8 wave (8λ) cavity design consisting of a 2λ AlGaInP active region surrounded by 3λ -doped AlInP cladding layers [2, 3]. Although previous attempts at employing a shorter cavity design [4] have not been as successful, an optimised 1λ cavity structure is expected to provide improved current injection efficiency and reduced cavity losses over the longer cavity designs. In this Letter, we report record performance from AlGaInP-based VCSELs employing a 1λ cavity design which eliminates the AlInP spacer layers.

The AlGaInP-based heterostructures were grown by MOVPE on <311> oriented GaAs substrates without wafer rotation as described previously [2]. The bottom DBR consists of 55 $1/2$ pairs of alternating Si doped ($n = 2 \times 10^{18} \text{cm}^{-3}$) 0.15λ -thick $\text{Al}_{0.3}\text{Ga}_{0.5}\text{As}$ and AlAs layers with 0.1λ -thick continuously parabolically graded transition layers ($x = 0.5-1$) at each interface. The top p -DBR has 34 periods and is carbon doped to $\sim 2 \times 10^{18} \text{cm}^{-3}$, with lower doping ($5-10 \times 10^{17} \text{cm}^{-3}$) near the cavity for reduced free carrier absorption and higher doping ($5-10 \times 10^{18} \text{cm}^{-3}$) in the top DBR

for improved contact resistance. The active region, centred in a 1λ cavity, consists of four 60\AA compressively strained $\text{In}_{0.56}\text{Ga}_{0.44}\text{P}$ quantum wells with 60\AA $(\text{Al}_{0.5}\text{Ga}_{0.5})_{0.3}\text{In}_{0.3}\text{P}$ barriers and $(\text{Al}_{0.5}\text{Ga}_{0.5})_{0.3}\text{In}_{0.3}\text{P}$ cladding layers. The active region is nominally undoped.

Planar gain guided lasers were fabricated in a top emitting geometry. A $100 \times 100\mu\text{m}^2$ AuBe top contact with a circular aperture in the centre was fabricated by lift-off techniques. Proton implantation was used to channel current into the aperture region of the device. The implant aperture diameters ranged from 5 to $50\mu\text{m}$. The devices were further defined into $100 \times 100\mu\text{m}^2$ mesas with a BCL_2/Cl_2 plasma etch through the top DBR. Light output against current (L-I) and current voltage (I-V) measurements were performed at room temperature under CW conditions by direct wafer probing. The devices were tested with the sample mounted substrate down on a heatsink held at 20°C . Because the wafer was not rotated during growth, there exists an approximately linear variation in emission wavelengths across the wafer. CW room temperature lasing was observed from lasers emitting at $661\text{--}681\text{nm}$ with the highest output powers achieved from lasers emitting at 676nm .

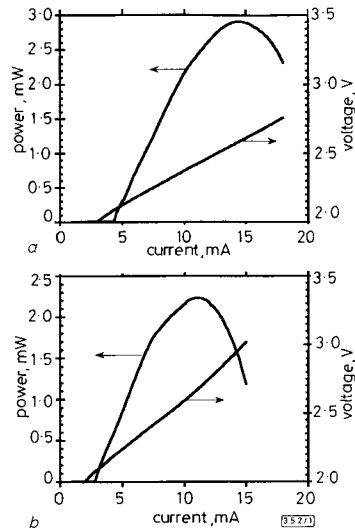


Fig. 1 Continuous wave light output power against current and current against voltage characteristics at 20°C of 1-wave cavity VCSELs with $20\mu\text{m}$ diameter implant aperture and $16\mu\text{m}$ diameter contact aperture, and $15\mu\text{m}$ diameter implant aperture and $11\mu\text{m}$ diameter contact aperture
a $20\mu\text{m}$ implant, $16\mu\text{m}$ contact aperture
b $15\mu\text{m}$ implant, $11\mu\text{m}$ contact aperture

In Fig. 1a, we show L-I and I-V data for a device emitting at 676nm with $20\mu\text{m}$ implant diameter and a $16\mu\text{m}$ diameter metal contact aperture. The device demonstrates a threshold current of 4.2mA and a low threshold voltage of 2.1V . A peak output power of 2.9mW is achieved at 14.3mA . Peak wallplug efficiency is 9% . In Fig. 1b, we show the L-I and I-V data for a device from the same region of the wafer with a $15\mu\text{m}$ implant aperture and an $11\mu\text{m}$ diameter metal aperture. While this device exhibits a lower output power of 2.24mW , the threshold current of 2.8mA and record low threshold voltage of 2.08V combine to yield a peak wallplug efficiency of 10% .

These results represent a substantial improvement over the best planar implanted 8λ cavity AlGaInP VCSELs, where a peak output power of 0.33mW and wallplug efficiency of $\sim 1\%$ were reported for a $25\mu\text{m}$ implanted device [2] [Note 1]. Direct evaluation of the effect of cavity length on the performance of the devices is made difficult by variations in the active region and DBR reflectivity for the two designs: the present 1λ cavity lasers employ four 60\AA $\text{In}_{0.56}\text{Ga}_{0.44}\text{P}$ quantum wells with 34 top DBR

Note 1: This represents the best performance for AlGaInP-based 8λ cavity VCSELs with AlGaAs DBRs. Slightly improved performance (0.52mW) was achieved from 8λ AlGaInP-based VCSELs with a partial dielectric top DBR: [5]

pairs while the 8λ cavity lasers had three 80\AA $\text{In}_{0.56}\text{Ga}_{0.44}\text{P}$ quantum wells with 36 top DBR pairs.

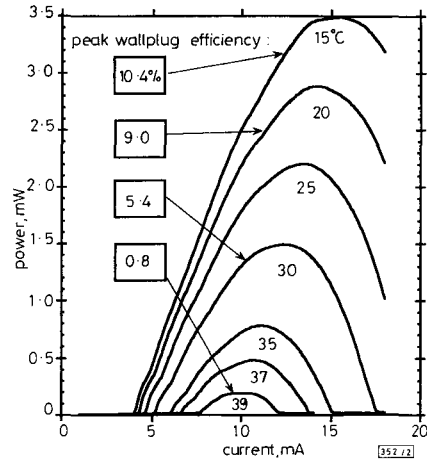


Fig. 2 Continuous wave light output power against current for $20\mu\text{m}$ diameter VCSEL at various heatsink temperatures

The peak wallplug efficiency at selected temperatures is indicated

In Fig. 2, we show L-I data for the same $20\mu\text{m}$ diameter laser at various heatsink temperatures. While the laser demonstrates a high output power of 3.5mW at 15°C , the power and efficiency drop with temperature, yielding a total output power of $200\mu\text{W}$ at 39°C . This thermal sensitivity is in part due to the misalignment of the peak gain and cavity mode with increasing temperature and may also be strongly affected by leakage currents. The detrimental effect of carrier leakage has been studied in AlGaInP-based edge emitting laser diodes and is attributed to the relatively small band offsets of these materials [6]. Efforts are currently underway to improve the high temperature performance of these visible VCSELs.

In conclusion, we have demonstrated enhanced performance of AlGaInP-based visible VCSELs with the application of a 1λ cavity design. Maximum multimode output power of 2.9mW and wallplug efficiency of 10% have been achieved from lasers emitting at 676nm , representing nearly an order of magnitude improvement over previously reported planar implanted visible VCSEL performance. With these advances, the AlGaInP-based VCSELs are fast approaching the performance levels required for a number of critical optoelectronics applications requiring visible laser light sources.

Acknowledgments: The authors acknowledge fruitful discussions with W. W. Chow, G. R. Hadley, I. J. Fritz, A. Owyong, J. Y. Tsao and S. T. Picraux as well as the technical assistance of S. Samora. This work is supported by the US Department of Energy under contract no. DE-AC04-94AL85000.

© IEE 1995
Electronics Letters Online No: 19950124

16 November 1994

M. Hagerott Crawford, R.P. Schneider, Jr., K.D. Choquette, K.L. Lear, S.P. Kilcoyne and J.J. Figiel (*Sandia National Laboratories, Albuquerque, NM 87185-0603, USA*)

References

- LOTT, J.A., SCHNEIDER, R.P., CHOQUETTE, K.D., KILCOYNE, S.P., and FIGIEL, J.J.: 'Room temperature continuous wave operation of red vertical cavity surface emitting laser diodes', *Electron. Lett.*, 1993, **29**, pp. 1693-1694
- SCHNEIDER, R.P., CHOQUETTE, K.D., LOTT, J.A., and LEAR, K.L.: 'Efficient room temperature continuous-wave AlGaInP/AlGaAs visible (670nm) vertical-cavity surface-emitting laser diodes', *IEEE Photonics Technol. Lett.*, 1994, **5**, pp. 313-316
- CHOQUETTE, K.D., SCHNEIDER, R.P., and LOTT, J.A.: 'Lasing characteristics of visible AlGaInP/AlGaInP vertical-cavity lasers', *Opt. Lett.*, 1994, **19**, pp. 969-971

- 4 HUANG, K.F., TAI, K., WU, C.C., and WYNN, J.D.: 'Continuous wave visible InGaP/InGaAlP quantum well surface emitting laser diodes', *Electron. Lett.*, 1993, **29**, pp. 1314-1315
- 5 LOTT, J.A., SCHNEIDER, R.P., MALLOY, K.J., KILCOYNE, S.P., and CHOQUETTE, K.D.: 'Red vertical cavity surface emitting laser arrays with partial top dielectric stack distributed Bragg reflectors', submitted to *IEEE Photonics Technol. Lett.*
- 6 BOUR, D.P., TREAT, D.W., THORNTON, R.L., GEELS, R.S., and WELCH, D.F.: 'Drift leakage current in AlGaInP quantum-well lasers', *IEEE J. Quantum Electron.*, 1993, **QE-29**, pp. 1337-1342

Highly reliable operation of strain-compensated 0.98 μm InGaAs/InGaP/GaAs lasers with InGaAsP strained barriers for EDFAs

T. Toyonaka, M. Sagawa, K. Hiramoto, K. Shinoda, K. Uomi and A. Ohishi

Indexing terms: Semiconductor junction lasers, Semiconductor quantum wells, Reliability

Highly reliable operation of 0.98 μm strain-compensated InGaAs/InGaAsP lasers is demonstrated for the first time with an estimated lifetime of 170kh at 25°C. Moreover, we reveal that the degradation rates at 90°C and 80mW output power are four times smaller than those of identical lasers with GaAs barriers.

Introduction: InGaAs strained quantum well (QW) lasers emitting at a 0.98 μm wavelength are considered to be indispensable components for pumping light sources for low-noise Er-doped fibre amplifiers (EDFAs). Realising high reliability for over 100kh is a key issue in applications to practical optical fibre systems. To begin with, sudden catastrophic failures due to facet degradation during laser operation have to be prevented. From this point of view, Al-free lasers [1-4] have an advantage over AlGaAs lasers because the oxidation-induced facet degradation is much lower in the Al-free lasers. Therefore, we have investigated Al-free InGaAs/InGaP/GaAs lasers and reported high-power operation [3]. In addition, with respect to the suppression of gradual degradation, crystal quality in the strained QW active layers has to be considered, especially in the case of 0.98 μm lasers, in which the InGaAs wells are under heavy compressive strain of over 1%. Lattice distortions have been observed in multiquantum well (MQW) structures with InGaAs wells under compressive strain and GaAs barriers [5]. With strain-compensated MQW structures, where the barriers are grown so as to be under tensile strain, superior CW performance, e.g. low threshold current densities and high characteristic temperatures, has been demonstrated [4]. For 0.98 μm lasers, in the case of Al-free InGaAs/InGaP/GaAs systems, strain-compensated QWs with InGaAsP strained barriers are adaptable [4]. This is impossible with AlGaAs lasers because AlGaAs is almost lattice-matched to GaAs ($\Delta a/a < 0.05\%$). However, as far as we know, there have been no reports on the reliability of such strain-compensated 0.98 μm lasers. In this Letter, we demonstrate highly reliable operation of 0.98 μm Al-free strain-compensated InGaAs/InGaAsP lasers for the first time. Assuming an activation energy of 0.4eV and a linear increase in operating current, the extrapolated lifetime is estimated to be 170kh at room temperature (25°C). Moreover, we reveal that the degradation rates at 90°C and 80mW output power are four times smaller than those of identical lasers with GaAs barriers.

Device structure: Fig. 1 shows a schematic cross-section of a buried ridge laser [3]. It consists of epitaxial layers grown on an n-GaAs substrate by low-pressure metalorganic vapour phase epitaxy (MOVPE). The GaAs waveguide layer, whose refractive index is higher than that of the InGaP cladding layers, provides a low-loss real-index waveguide. The active layer consists of a 7 nm InGaAs well under 1.4% compressive strain sandwiched by two 10 nm InGaAsP barriers ($E_g = 1.61\text{eV}$) under 0.3% tensile strain and two 25 nm InGaAsP unstrained SCH layers ($E_g = 1.61\text{eV}$). Identical

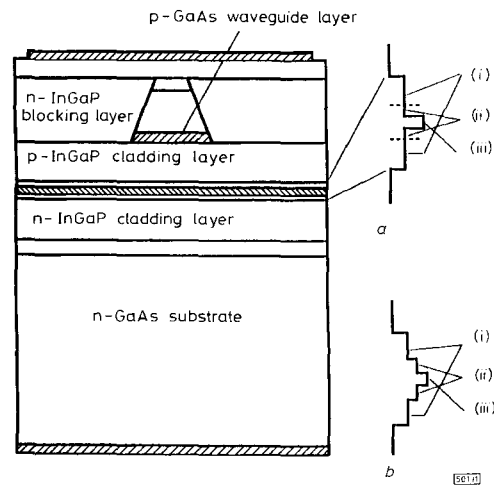


Fig. 1 Schematic cross-section of a buried ridge laser

a InGaAs strained QW with InGaAsP barriers

- (i) InGaAsP, 25 nm, $E_g = 1.61\text{eV}$
- (ii) InGaAsP barrier, 10 nm, $E_g = 1.61\text{eV}$, $\Delta a/a = -0.3\%$
- (iii) InGaAs well, 7 nm, $\Delta a/a = 1.4\%$

b InGaAs strained QW with GaAs barriers

- (i) InGaAsP, 20 nm, $E_g = 1.57\text{eV}$
- (ii) InGaAs barrier, 8 nm
- (iii) InGaAs well, 7 nm, $\Delta a/a = 1.4\%$

cal lasers with GaAs barriers were also fabricated for comparison. The active layer is shown in Fig. 1. The optical confinement factors of these lasers were designed to be the same. The cavity length was 900 μm . The laser chips were mounted on heatsinks with their junctions down.

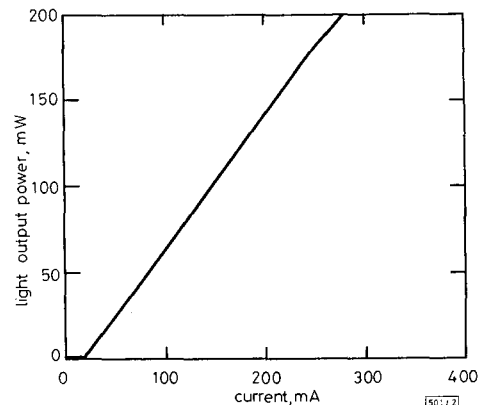


Fig. 2 Light output power against current characteristics of laser with InGaAsP barriers

25°C, CW; threshold current = 17mA at 25°C

Characteristics and reliability: Fig. 2 shows the CW light output power against current (L/I) characteristics of the laser with InGaAsP barriers. The threshold current (I_{th}) was 17mA at 25°C. Singlemode operation with no kink was maintained up to 180mW. The vertical and lateral full-width at half-maxima of the far-field pattern at 80mW output power were 30 and 10°, respectively. The lasing wavelength at 25°C and 80mW output power was 0.978 μm , which matched the pumping band of EDFAs.

Fig. 3 shows the extended lifetest results at 80-120mW output power in constant power mode at 50°C. All the lasers exhibit stable operation without sudden failures. Long-term lifetests at three different elevated temperatures have been carried out to determine the degradation rates and activation energy. Fig. 4 shows the degradation rates after 1kh ($\Delta I/I$) under 80mW output power in constant power mode at 50, 70 and 90°C. The activation energy of